# Effect of temperature on $In_xGa_{1-x}As$/GaAs quantum dots

MAHDI AHMADI BORJI[1], ALI REYAHI[2,3], ESFANDIAR RAJAEI[4,*]
and MOHSEN GHAHREMANI[2]

[1]Department of Physics, Payame Noor University (PNU), P.O. Box 19395-3697, Tehran, Iran
[2]Laser and Optics Research Center, Imam Hossein University, Tehran, Iran
[3]Department of Physics, Iran University of Science and Technology, Tehran, Iran
[4]Department of Physics, University of Guilan, Namjoo Street, Rasht, Iran
*Corresponding author. E-mail: Raf404@guilan.ac.ir

**Abstract.** In this paper, the strain, band-edge, and energy levels of pyramidal $In_xGa_{1-x}As$/GaAs quantum dots are investigated by 1-band effective mass approach. It is shown that while temperature has no remarkable effect on the strain tensor, the band gap lowers and the radiation wavelength elongates by increasing temperature. Also, band gap and energy do not linearly decrease by temperature rise. Our results appear to agree with former researches. This can be used in designing laser devices and sensors when applied in different working temperatures. Furthermore, when the device works for a long time, self-heating occurs which changes the characteristics of the output.

## 1. Introduction

Semiconductor lasers are the most important lasers that are used in cable television signals, telephone and image communications, computer networks and interconnections, CD-ROM drivers, reading barcodes, laser printers, optical integrated circuits, telecommunications, signal processing, and a large number of medical and military applications. Quantum dot semiconductor lasers, due to the discrete density of states, low threshold current and temperature dependence, high optical gain and quantum efficiency and high modulation speed, are superior to other lasers [1]. Effects of various factors such as temperature [2–5], size of the quantum dots [6–8], stoichiometric percentage of constituent elements of the laser active region [9–12], substrate index [13,14], strain effect [15,16], wetting layer (WL), and distribution and density of quantum dots are shown to be important in the energy levels and performance of QDLs. Therefore, finding the functionality of the impact of these factors can help in optimizing the performance of quantum dot lasers. Attention should be given to the effects of temperature, as adverse effects that can happen by the change in working conditions should be predicted.

QD nanostructures have been the focus of many investigations due to their optical properties arising from the quantum confinement of electrons and holes [17–20]. By now, QD materials have found very promising applications in sensors, optical amplifiers, and semiconductor lasers [21–24]. Therefore, having a ubiquitous view of energy states, strain, and other physical features, and their change by varying some factors such as temperature is instructive. Based on this fact, many research groups attempt to develop and optimize QDs to fabricate optoelectronic devices with better performance.

Finding a way to enhance the efficiency of a QD with fixed size can be helpful. Among many materials, InGaAs/GaAs devices have attracted many scientists due to their interesting features [20,25–29]. However, sensors or lasers may be used in very low [5,30,31] or high [32,33] temperature conditions which will affect their work. Also it is proved that temperature affects the lasing process through both the change of output photoluminescence and the laser characteristics [5] because the behaviour of the carriers depends on temperature.

In semiconductor (SC) heterostructures containing two or more semiconductors with different lattice constants, band edge diagrams show more complexity than the usual bulk semiconductors because of the

important role of strain. Strain tensor depends on the elastic properties of neighbour materials, lattice mismatch, and geometry of the quantum dot [34].

Rouillard *et al* [33] worked on high-temperature effects on mid-infrared semiconductor laser. Tong *et al* [31] studied InAs/GaAs QDLs at negative characteristic temperature but at fixed energy levels. Rossetti *et al* [5] investigated the effect of temperature on carrier lifetime, laser threshold current, radiative and differential efficiency, and gain after assuming the energies as constants. Temperature-independent strain was shown in Sung Chul *et al* [35] and the sensitivity of the strain was found in [36].

This research will numerically study the band structure and strain tensor of $In_xGa_{1-x}As$ quantum dots grown on GaAs substrate to look for more efficient QDs by changing the working temperature.

The rest of this paper is organized as follows: Section 2 explains the model and method of the numerical simulation. Our results and discussions on the temperature effects are presented in §3. Finally, we draw a conclusion in §4.

## 2. Modelling and numerical simulation of the effective mass tensor

Band structure of the zinc-blende crystal can be obtained through:

$$(H_0 + H_k + H_{k.p} + H_{s.o.} + H'_{s.o.})u_{n\mathbf{k}}(\mathbf{r}) = E_n(\mathbf{k})\,u_{n\mathbf{k}}(\mathbf{r}), \tag{1}$$

where $u_{n\mathbf{k}}(\mathbf{r})$ is a periodic Bloch spinor (i.e., $\psi_{n\mathbf{k}}(\mathbf{r}) = e^{i\mathbf{k}.\mathbf{r}}u_{n\mathbf{k}}(\mathbf{r})$) and

$$H_0 = \frac{\mathbf{p}^2}{2m_0} + V_0(\mathbf{r}, \varepsilon_{ij}), \tag{2}$$

$$H_k = \frac{\hbar^2\mathbf{k}^2}{2m_0}, \tag{3}$$

$$H_{k.p} = \frac{\hbar}{m_0}\mathbf{k} \cdot \mathbf{p}, \tag{4}$$

$$H_{s.o.} = \frac{\hbar}{4m_0^2c^2}(\boldsymbol{\sigma} \times \nabla V_0(\mathbf{r}, \varepsilon_{ij})) \cdot \mathbf{p}, \tag{5}$$

$$H'_{s.o.} = \frac{\hbar}{4m_0^2c^2}(\boldsymbol{\sigma} \times \nabla V_0(\mathbf{r}, \varepsilon_{ij})) \cdot \hbar\mathbf{k}. \tag{6}$$

Here, $V_0(\mathbf{r}, \varepsilon_{ij})$ is the periodic potential of the strained crystal, $\boldsymbol{\sigma} = (\sigma_x, \sigma_y, \sigma_z)$ is the Pauli spin matrix, $c$ is the light velocity, and $m_0$ is the mass of the electron. This equation can be solved by the expansion of $V_0(\mathbf{r}, \varepsilon_{ij})$ to

first order in the strain tensor $\varepsilon_{ij}$. Taking into account the change in length in all directions, one achieves the strain tensor as

$$\varepsilon_{ij} = \frac{1}{2}\left(\frac{\mathrm{d}u_i}{\mathrm{d}r_j} + \frac{\mathrm{d}u_j}{\mathrm{d}r_i}\right), \ i, j \equiv x, y, z, \tag{7}$$

where $\mathrm{d}u_i$ is the change in length in the $i$th direction and $r_j$ is the length in the direction $j$ [13]. The resulting equation for a strained structure is then

$$\left(H_0 + \frac{\hbar^2\mathbf{k}^2}{2m_0} + \frac{\hbar}{m_0}\mathbf{k} \cdot \mathbf{p}'\right)u_{n\mathbf{k}}(\mathbf{r}) = E_n(\mathbf{k})u_{n\mathbf{k}}(\mathbf{r}) \tag{8}$$

where

$$\mathbf{p}' = \mathbf{p} + \frac{\hbar}{4m_0c^2}(\boldsymbol{\sigma} \times \nabla V_0(\mathbf{r}, \varepsilon_{ij})). \tag{9}$$

For detailed explanation we refer the reader to [37]. This equation can be solved by the second-order non-degenerate perturbation scheme in which the latter terms are considered as the perturbation. Therefore, in the Cartesian space, the solution is

$$E_n(\mathbf{k}) = E_n(\mathbf{0}) + \frac{\hbar^2k_ik_j}{2}\left(\frac{1}{m_n^*}\right)_{i,j} \tag{10}$$

in which the tensor of the effective mass is defined as

$$\left(\frac{1}{m_n^*}\right)_{i,j} = \left(\frac{1}{m_0}\right)\delta_{i,j}$$
$$+ \frac{2}{m_0^2}\sum_{m\neq n}\frac{\langle n, 0|p_i'|m, 0\rangle\langle m, 0|p_j'|n, 0\rangle}{E_n(0) - E_m(0)} \tag{11}$$

and $i, j \equiv x, y, z$. Also, for $In_xGa_{1-x}As$, the parameters are calculated as follows:

Lattice constant at $T = 300$ K [38]:

$$a = (6.0583 - 0.405(1 - x)) \text{ Å}. \tag{12}$$

Effective electron mass at 300 K [39]:

$$m_e = (0.023 + 0.037(1 - x) + 0.003(1 - x)^2)m_0. \tag{13}$$

Effective hole mass at 300 K [40]:

$$m_h = (0.41 + 0.1(1 - x))m_0. \tag{14}$$

Effective light-hole masses at 300 K:

$$m_{lp} = (0.026 + 0.056(1 - x))m_0. \tag{15}$$

Effective split-off band hole masses at 300 K is $\sim 0.15m_0$.

In self-assembled $In_xGa_{1-x}As$ QDs, the first WL with a few molecular layers is grown on the substrate,
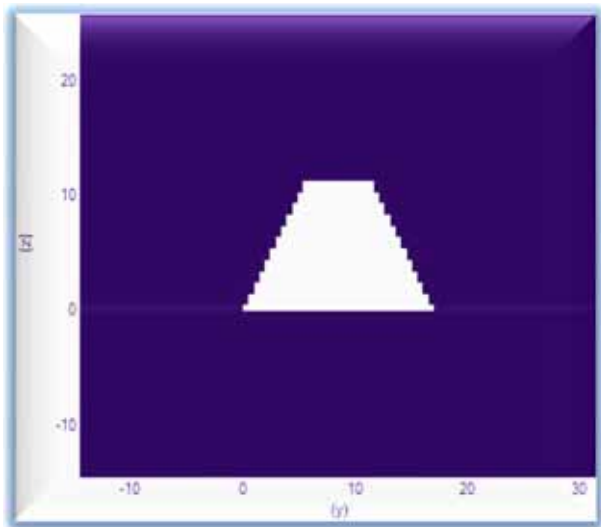
**Figure 1.** Cross-section of a pyramidal InGaAs QD with a square base of 17 nm × 17 nm area and the height is 2/3 times the base width on 15 nm thick GaAs substrate and 0.5 nm wetting layer.

and then, millions of QD islands grow on the wetting layer, with each having a random shape and size. The resulting system is finally covered by GaAs. Many shapes can be approximated for QDs, namely cylindrical, cubic, lens shape, pyramidal [41], etc. QDs are supposed to be far enough not to be influenced by other QDs. The one-band effective mass approach is used for solving the Schrödinger equation.

Figure 1 shows the profile of a pyramidal $In_{0.4}Ga_{0.6}As$ QD surrounded by a substrate and cap layer of GaAs [7]. This composition of indium and gallium is used in laser devices [42]. Both GaAs and InAs have zincblende structure. The pyramid has a square base of 17 nm × 17 nm area and the height is 2/3 times the base width on 15 nm thick GaAs substrate and 0.5 nm wetting layer. This structure is grown on (0 0 1) substrate index. As can be observed from the picture, WL

is much thinner than QD height. The growth direction of the structure is $z$.

The parameters related to the bulk materials used in this work are given in table 1; the data are extracted from refs [43–45].

## 3. Results and discussion

Strain is generally defined as the increase in length relative to the initial length ($\varepsilon_L = \Delta L/L$) or the summation of all infinitesimal increases in length relative to the instantaneous lengths ($\varepsilon_L = \sum \Delta L_t/L_t$). The diagonal elements of the strain tensor are related to expansions along an axis (stretch), but the off-diagonal elements represent rotations. This tensor is symmetric (i.e., $\varepsilon_{ij} = \varepsilon_{ji}$) although the distortion matrix **u** may be non-symmetric. In our case, the strain tensor is a diagonal matrix as follows:

$$\varepsilon = \begin{bmatrix} \varepsilon_{xx} & 0 & 0 \\ 0 & \varepsilon_{yy} & 0 \\ 0 & 0 & \varepsilon_{zz} \end{bmatrix} \quad (16)$$

in which $\varepsilon_{xx} = \varepsilon_{yy}$ due to the symmetry. This tensor shows a biaxial in-plain strain defined as

$$\varepsilon_{xx} = \varepsilon_{yy} = \varepsilon_{||} = \frac{a_{||} - a_{\text{substrate}}}{a_{\text{substrate}}} \quad (17)$$

and a perpendicular uniaxial strain defined as [46]

$$\varepsilon_{zz} = \varepsilon_{\perp} = -\frac{2C_{xy}}{C_{xx}}\varepsilon_{xx} = \frac{a_{\perp} - a_{\text{substrate}}}{a_{\text{substrate}}}, \quad (18)$$

where $C_{ij}$ are components of the matrix which interconnect stress $\sigma$ to strain (i.e., $\sigma = C\varepsilon$) [47]. In figures 2a and 2b variation of strain is illustrated in different points of the middle cross-section of the structure. As can be

**Table 1.** Parameters used in the model.

| Parameters used | GaAs | InAs |
|---|---|---|
| Band gap (0 K) | 1.424 eV | 0.417 eV |
| Lattice constant | 0.565325 nm | 0.60583 nm |
| Expansion coefficient of lattice constant | 0.0000388 | 0.0000274 |
| Effective electron mass ($\Gamma$) | $0.067m_0$ | $0.026m_0$ |
| Effective heavy hole mass | $0.5m_0$ | $0.41m_0$ |
| Effective light hole mass | $0.068m_0$ | $0.026m_0$ |
| Effective split-off mass | $0.172m_0$ | 0.014 |
| Nearest-neighbour distance (300 K) | 0.2448 nm | 0.262 nm |
| Elastic constants | $C_{11} = 122.1$ | $C_{11} = 83.29$ |
|  | $C_{12} = 56.6$ | $C_{12} = 45.26$ |
|  | $C_{44} = 60$ | $C_{44} = 39.59$ |
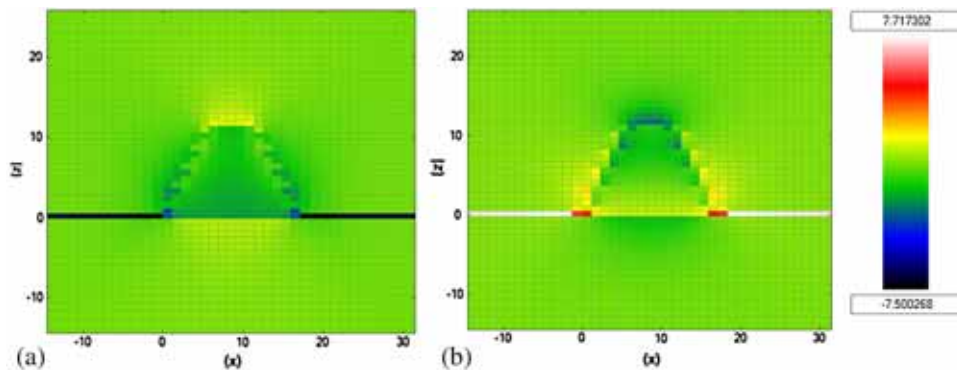
**Figure 2.** Strain tensor along the $x$ and $z$ directions in different points of the device at $T = 300$ K.
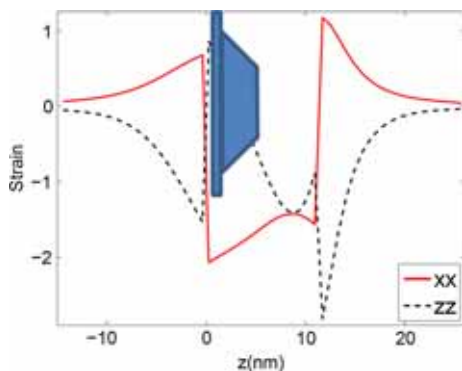


**Figure 3.** Non-zero elements of the strain tensor at $T = 300$ K.

seen, strain tensor is subjected to change in both the directions. However, obviously, most of the variations are viewed at interfaces.

In figure 3, the non-zero elements of the strain tensor are drawn by going up through $z$-direction and at the middle of the structure. It can be noticed that the existence of indium on one side of the interface has caused a jump in the strain tensor for $\varepsilon_{xx}$ ($\varepsilon_{yy}$) and $\varepsilon_{zz}$, meaning a tension in GaAs and compression in InGaAs lattice constants. This figure was found to be the same for different values of working temperature. This shows that change in temperature has no effect on the strain tensor.

This result seems logical, as it was proved that strain is only dependent on the ratio of lattice constants which linearly changes with temperature (i.e., $a = b(T - 300) + a_{300K}$). So, their ratio remains fixed and strain does not change by temperature. This means that our result can be acceptable from analytical point of view.

Figures 4a–4d show the band edge of each point of the pyramidal QDs at 300 K for $\Gamma$, heavy-hole
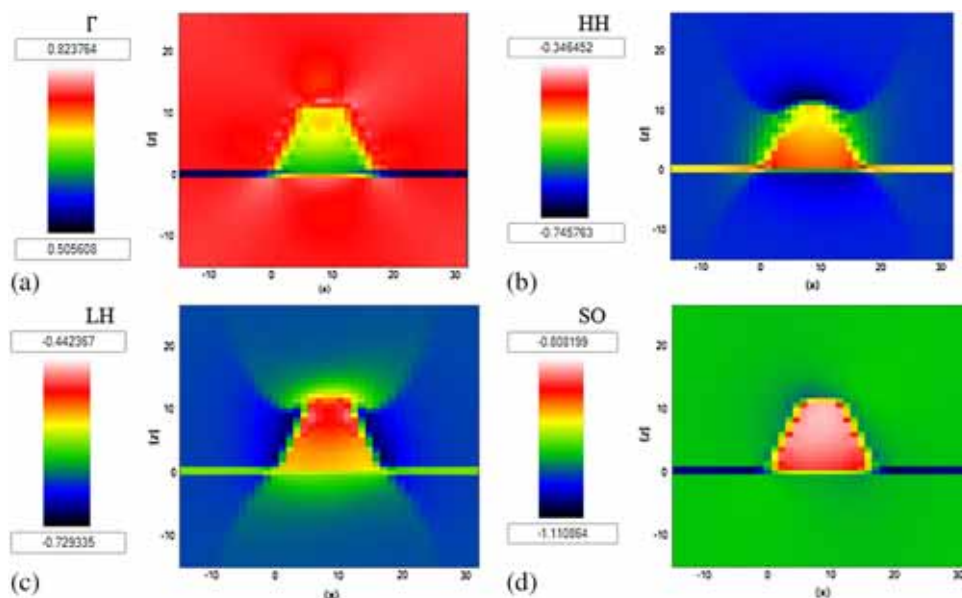


**Figure 4.** Valence and conduction band edges in $x-y$ plane in the central point of the QD at $T = 300$ K. Note the numbers related to colours beside each figure.
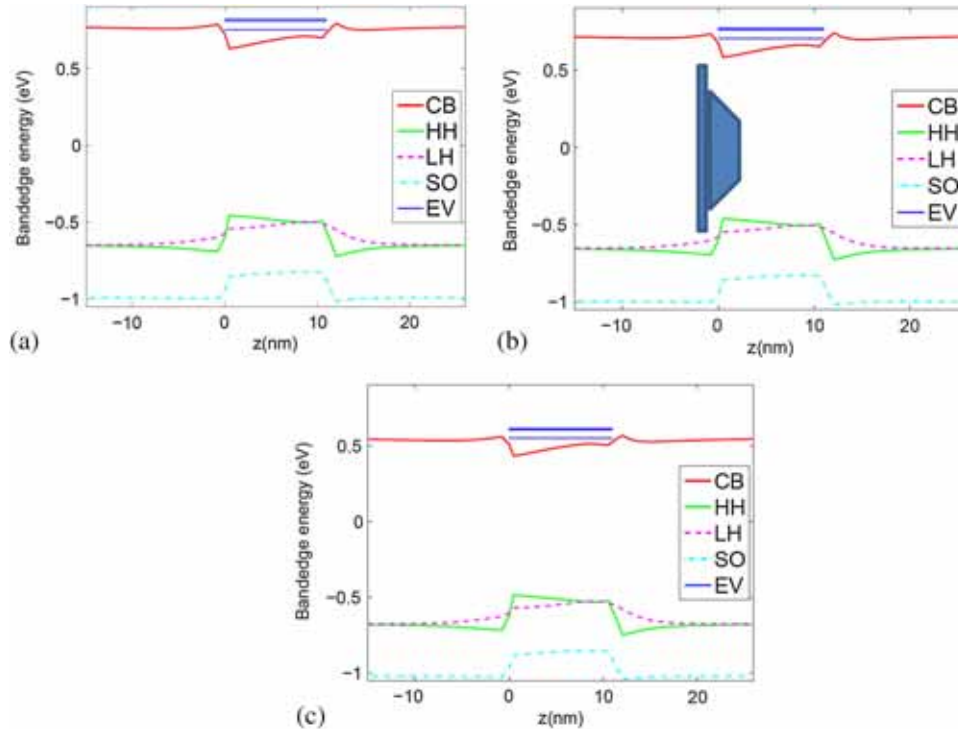
**Figure 5.** Conduction and valence Γ band edges of QDs in the *z*-direction along with the three first allowed energy states for electrons at different temperatures. All heavy-hole (HH), light-hole (LH), and split-off (SO) band edges can also be seen in the valence band. (**a**) $T = 300$ K, (**b**) $T = 400$ K, (**c**) $T = 700$ K.

(HH), light-hole (LH), and split-off (SO) respectively. Both GaAs and InAs have direct band gaps. As can be seen, the band edges change in different points. Figure 4a indicates that the energy difference is the biggest at the deepest points into the QD with the cap layer. Also, the cap layer band edges have been subjected to change in the points close to the QD. Also, figures 4b–4d show hole band-edges which have less values; nevertheless, their band edges are different which can be explained as due to the changes in the effective masses, because heavy hole band has the largest, and split-off band has the smallest effective mass. All the figures show symmetry through *x*-axis. Moreover, the figures show that band energy of the corners of the QD have matched their energy more than other points.

In figure 5 snapshots for conduction and valence Γ band edges are shown in the *z*-direction, and the three first allowed energy states for electrons and holes are pointed out. All HH, LH, and SO band edges can also be seen in the valence band.

It is seen that in the physical conditions mentioned, the first electronic eigenvalue separates from higher continuous states and goes down into the QD. This energy state is the ground-state (GS) atom-like electron state with its special energy level which can

be used in the recombination energy of electrons and holes. Other states are among the continuous states of GaAs.

However, the dependence of band edges and energies on temperature is an interesting phenomenon. Obviously, by increasing the temperature from 300 K to 700 K, the GS levels of electrons have been displaced. The electronic states appear to decrease from 0.75 eV to 0.55 eV, showing that the e-h energy difference changes by changing the temperature. This leads to different wavelengths of the QD laser. In the same way, it can be observed that all the band edges and the band gaps have been temperature-sensitive.

Moreover, figure 6 gives a comparison of band edge for different temperature. Obviously, effect of temperature on the band edges is remarkable in a wide range of temperature. As can be seen, rise of temperature has lowered the band edges of both the substrate and the quantum dot.

Functionality of energy gap by change of temperature is shown to be

$$E_g = E_{g(T=0)} - 5.405 \times 10^{-4} \frac{T^2}{T + 204}$$

and

$$T \in [0, 1000] \tag{19}$$
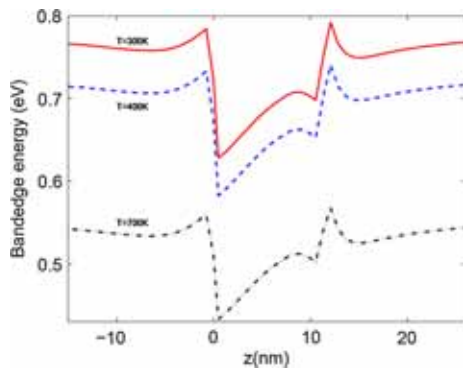
**Figure 6.** Comparison of Γ-band edges at different temperatures.
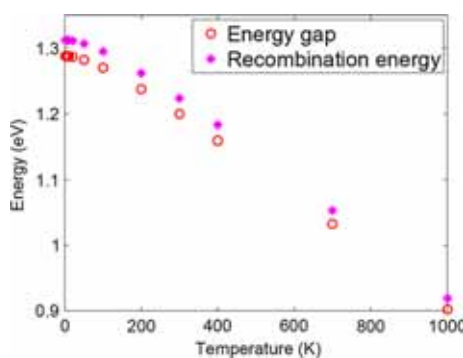


**Figure 7.** Energy gap and recombination energy of the first electron and hole eigenvalues at different temperatures.

for GaAs and

$$E_g = E_{g(T=0)} - 2.76 \times 10^{-4} \frac{T^2}{T + 83}$$

and

$$T \in [0, 300] \tag{20}$$

for InAs, in which $E_g$ is in eV and $T$ is in Kelvin [48]. Also, for different compositions of indium and gallium in $Ga_x In_{1-x} As$, the behaviour of energy gap is [49]

$$E_g(x) = 0.36 + 0.63x + 0.43x^2 \quad \text{and } T = 300 \text{ K} \tag{21}$$

$$E_g(x) = 0.4105 + 0.6337x + 0.475x^2 \quad \text{and } T = 2 \text{ K}. \tag{22}$$

The melting point for GaAs and InAs is respectively 1511 K and 1215 K. In figure 7, the energy gap and recombination energy of the first eigenvalue are plotted as a function of temperature for a wide temperature range. This range was previously used for bulk materials in ref. [48]. Although all the temperatures are not viable, as the laser structure corrupts in hot conditions, the behaviour represents the effect of temperature. Interestingly, impact of temperature on energies is not linear,

which is the most important conclusion of this paper. Decrease in recombination energy results in increase in laser wavelength which must be paid attention in the lasers.

Comparison of these results which are related to bulk semiconductors show that our results can be logical. As can be inferred, our results are almost similar to the results found for bulk samples.

## 4. Conclusion

We investigated the band structure and strain tensor of $In_x Ga_{1-x} As$ QDs grown on GaAs substrate by quantum numerical solution. It was shown that under normal conditions, rise in temperature does not change strain tensor, but it slightly decreases the conduction and valence band edges as well as electron- and hole-energy states. Moreover, the main result was that temperature does not have a linear impact on the band-gap and recombination energies; both decrease as temperature increases. This reality can be used in the fabrication of sensors, solar cells, and laser devices when applied in different working temperatures. Also, self-heating of the laser device, if the working time is long, changes the features of its output light, which must be taken into account when a good lasing is aimed.

## References

[1] M Qorbani, E Rajaei, O Hajizadeh and M A Borji, *Iran. J. Sci. Technol. Trans. A: Sci.* **1** (2017)

[2] S H Chen and J-L Xiao, *Int. J. Mod. Phys. B* **21**, 5331 (2007)

[3] D Kumar, C M S Negi and J Kumar, Temperature effect on optical gain of CdSe/ZnSe quantum dots, in: V Lakshminarayanan and I Bhattacharya (eds) *Advances in optical science and engineering* (Springer, India, 2015) p. 563

[4] M Narayanan and A J Peter, *Quantum Matter* **1**, 53 (2012)

[5] M Rossetti, A Fiore, G Sęk, C Zinoni and L Li, *J. Appl. Phys.* **106**, 023105 (2009)

[6] S Baskoutas and A F Terzis, *J. Appl. Phys.* **99**, 013708 (2006)

[7] C Pryor, *Phys. Rev. B* **57**, 7190 (1998)

[8] E Rajaei and M A Borji, *Int. J. Nanosci. Nanotechnol.* **12**, 45 (2016)

[9] Z Shi, L Huang, Y Yu, P Tian and H Wang, *Front. Optoelectron. China* **4**, 364 (2011)

[10] M A Borji and E Rajaei, *J. Nanoelectron. Optoelectron.* **11**, 315 (2016)

[11] M A Borji and E Rajaei, arXiv:1511.00999 [physics. comp-ph] (unpublished observations) (2015)

[12] M A Borji and E Rajaei, *Iran. J. Sci. Technol. Trans. A: Sci.* **1**, 1 (2016)

[13] M Povolotskyi, A Di Carlo, P Lugli, S Birner and P Vogl, *IEEE Trans. Nanotechnol.* **3**, 124 (2004)

[14] E Rajaei and M A Borji, arXiv:1511.00997 [physics. comp-ph] (unpublished observations) (2015)

[15] C E Pryor and M E Pistol, *Phys. Rev. B* **72**, 205311 (2005)

[16] M Shahraki and E Esmaili, *J. Theor. Appl. Phys.* **6**, 1 (2012)

[17] M Zíková and A Hospodková, Nanocon. 23, 10 (2012).

[18] Y J Ma, Z Zhong, X J Yang, Y L Fan and Z M Jiang, *Nanotechnol.* **24**, 015304 (2013)

[19] Z D Kaftroudi and E Rajaei, *J. Theor. Appl. Phys. (Iran. Phys. J.)* **4**, 12 (2010)

[20] R Nedzinskas, B Čechavičius, J Kavaliauskas, V Karpus, G Valušis, L Li, S P Khanna and E H Linfield, *Nanoscale Res. Lett.* **7**, 609 (2012)

[21] D Bimberg, M Grundmann, F Heinrichsdorff, N N Ledentsov, V M Ustinov, A E Zhukov, A R Kovsh, M V Maximov, Y M Shernyakov, B V Volovik, A F Tsatsul'nikov, P S Kop'ev and Z I Alferov, *Thin Solid Films* 367, 235 (2000).

[22] M Gioannini, *IEEE J. Quantum Electron.* **42**, 331 (2006)

[23] Z D Kaftroudi and E Rajaei, *Opt. Commun.* **284**, 330 (2011)

[24] L V Asryan and S Luryi, *IEEE J. Quantum Electron.* **37**, 905 (2001)

[25] J C Woolley, M B Thomas and A G Thompson, *Can. J. Phys.* **46**, 157 (1968)

[26] P Hazdra, J Voves, J Oswald, K Kuldová, A Hospodková, E Hulicius and J Pangrác, *Microelectron. J.* **39**, 1070 (2008)

[27] A Fali, E Rajaei and Z Kaftroudi, *J. Korean Phys. Soc.* 64, 16 (2014).

[28] Y Yekta Kiya, E Rajaei and A Fali, *J. Theor. Phys.* **1**, 246 (2012)

[29] A Shafieenezhad, E Rajaei and S Yazdani, *Int. J. Sci. Eng. Technol.* **3**, 297 (2014)

[30] Q Le-Van, X Le Roux, T V Teperik, B Habert, F Marquier, J J Greffet and A Degiron, *Phys. Rev. B* **91**, 085412 (2015)

[31] C Z Tong, S F Yoon and C Y Liu, *J. Appl. Phys.* **101**, 104506 (2007)

[32] R W Ohse, *Pure Appl. Chem.* **60**, 309 (1988)

[33] Y Rouillard, A N Baranov, D A Yarekha, A Perona, A Vicet, A Joullie and C Alibert, Laser and fiber-optical networks modeling, in: *Proceedings of the 2nd International Workshop on LFNM 2000*, pp. 6–8

[34] A Trellakis, T Zibold, T Andlauer, S Birner, R K Smith, R Morschl and P Vogl, *J. Comput. Electron.* **5**, 285 (2006)

[35] K Sung Chul, K Se Yoon, L Sang Bae, K Seo Won, C Sang Sam and L Byoungho, *IEEE Photon. Technol. Lett.* **10**, 1461 (1998)

[36] P-H Wu, Y-S Huang, H-P Hsu, C Li, S-H Huang and K-K Tiong, *Appl. Phys. Lett.* **104**, 241605 (2014)

[37] T B Bahder, *Phys. Rev. B* 41, 11992 (1990).

[38] S Adachi, *J. Appl. Phys.* **54**, 1844 (1983)

[39] T P Pearsall, *GaInAsP alloy semiconductors* (John Wiley and Sons, New York, 1982)

[40] Yu A Goldberg and N M Schmidt, World Scientific, London, **2**, 62 (1999)

[41] D Qiu and M X Zhang, *Scr. Mater.* **64**, 681 (2011)

[42] K Kamath, J Phillips, H Jiang, J Singh and P Bhattacharya, *Appl. Phys. Lett.* **70**, 2952 (1997)

[43] Y D Jang, U H Lee, H Lee, D Lee, J S Kim, J Y Leem and S K Noh, *J. Korean Phys. Soc.* **42**, 111 (2003)

[44] J Singh, *Physics of semiconductors and their heterostructures* (McGraw-Hill, NY, 1993).

[45] C Yu, *Fundamentals of semiconductors* (Springer, Berlin, 2010).

[46] M Peressi, N Binggeli and A Baldereschi, *J. Phys. D: Appl. Phys.* **31**, 1273 (1998)

[47] S L Chuang and C S Chang, *Semicond. Sci. Technol.* **12**, 252 (1997)

[48] Z M Fang, K Y Ma, D H Jaw, R M Cohen and G B Stringfellow, *J. Appl. Phys.* **67**, 7034 (1990)

[49] K H Goetz, D Bimberg, H Jürgensen, J Selders, A V Solomonov, G F Glinskii and M Razeghi, *J. Appl. Phys.* **54**, 4543 (1983)

[50] S Birner, T Zibold, T Andlauer, T Kubis, M Sabathil, A Trellakis and P Vogl, *IEEE Trans. Electron Devices* **54**, 2137 (2007)